Physics issues and simulation of the JT-60 SA divertor for large heat and particle handling

N. Asakura [1)], H. Kawashima[1)], K. Shimizu[1)], S. Sakurai[1)], T. Fujita[1)], H. Takenaga[1)], T. Nakano[1)], H. Kubo[1)], S. Higashijima[1)], T. Hayashi[1)], Y. Kamada[1)], S. Ide[1)], M. Kikuchi[1)], Y. Takase[2)], Y. Ueda[3)], N. Ohno[4)], M. Sakamoto[5)], O. Gruber[6)], A. Kallenbach[6)], A. Grosman[7)], M. Lipa[7)]

1) Japan Atomic Energy Agency, Naka, Japan,
2) Graduate School of Frontier Sciences, Univ. Tokyo,Japan,
3) Graduate school of Engineering, Osaka Univ., Japan,
4) EcoTopia Science Research Institute, Nagoya Univ., Japan,
5) Research Institute for Applied Mechanics, Kyushu Univ. Japan,
6) Max-Planck-Institut für Plasmaphysik, IPP-EURATOM Association, Garching, Germany,
7) Association EURATOM-CEA, Cadarache, France

1. Introduction

Design work of the JT-60SA divertor has been progressing in order to handle large heat flux (maximum injection power of 41MW) during 100 s [1]. Divertor geometry must be suitable for *ITER-like* and *high-*β_N plasma configurations, which have different triangularity and aspect ratio. At the same time, divertor components such as target plates, dome and cooling system are optimized to incorporate in compact cassettes for remote maintenance [2]. Lower single-null (LSN) divertor is design for the ITER-like plasma configuration as shown in Fig.1 (a). Design concept and simulation results of heat reduction and particle flow in the LSN divertor, using 2D fluid (plasma) and Monte-Carlo (neutral) codes, are summarized.

2. Design concept of the divertor

Figure 1(a) show a standard ITER-like plasma configuration: R_p/a^{mid}~3.1, κ_{95}=1.7, δ_{95}=0.27, q_{95}=3.0, S=4.2 for I_p = 3.5 MA, B_t=2.65 T. Figure 1(b) shows typical high shaping plasma: R_p/a^{mid}~2.65, κ_{95}=1.74, δ_{95}=0.41, q_{95}=3.37, S=5.7 for I_p = 5.5 MA, B_t=2.7 T, and the upper single-null (USN) divertor geometry will be optimized.

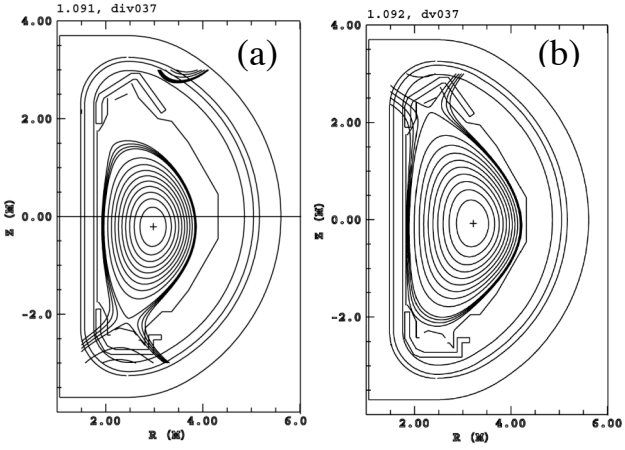

Fig.1 (a) Lower single-null divertor for ITER-like plasma (R_p/a^{mid}~3.1), (b) Upper single-null divertor for high shaping plasma (S~5.7) and low aspect ratio (R/a=2.65) configuration.

Physics concept of the ITER divertor is control of the plasma detachment. It is also the most important issue in JT-60SA in order to reduce large exhaust power. Figure 2(a) shows cross-section of the LSN divertor, where magnetic field lines at midplane distance from separatrix (ΔR^{mid}) of 0, 1, 2, 3 cm are drawn. Basic design concept for the divertor geometry is similar to ITER. (1) Vertical target is used to increase particle recycling

and radiation power efficiently along the divertor leg. (2) Dome is installed for ITER physics research: neutrals are pumped from the private region, and the inner and outer exhaust slots are connected under the dome. (3) The outer exhaust slot is allocated between 8 and 18 cm above the strike point, which will efficiently produce plasma detachment near the strike-point in the "V-shaped corner". (4) SOL plasma for ΔR^{mid} < 3 cm (width is larger than e-folding length of particle flux profile) is guided into the divertor. Here, small dome height is required to increase δ, κ and S of the USN plasma configuration as shown in Fig.1 (b).

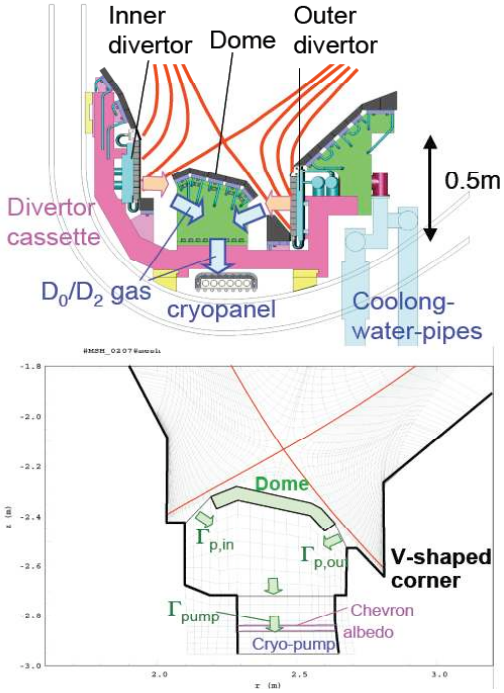

Fig.2 (a) Cross-section of lower divertor for ITER-like plasma configuration. (b) Calculation mesh for plasma and neutral transport codes and arrows illustrating the neutral recycling and pumping fluxes.

3. Power handling of the ITER-like divertor

Divertor heat load and neutral flow for the LSN divertor were evaluated, using 2D fluid plasma code (SOLDOR) and Monte-Carlo neutral code (NEUT2D) [3-5]. For the initial study, radiation power from carbon impurity is calculated by a simplified non-corona model [6], assuming residence parameter of $n_e\tau_{res}$ = $4x10^{15}$ $m^{-3}s$ (τ_{res} is the impurity residence time) and uniform carbon contamination (n_C/n_e) of 1 % in divertor and edge plasmas. Calculation mesh in the divertor is shown in Fig. 2(b). Core plasma boundary ("edge") is set at r/a =0.95, where power flux of Q_{out}=37 MW (assuming 4 MW loss in core) and ion flux of Γ_{out} = $5x10^{21}$ D/s are exhausted. Density profile of H-mode plasma is modeled with combination of particle diffusion coefficient, $D_\perp$, and pinch velocity, $v_\perp$, in inside-separatrix and SOL, i.e. $D_\perp$ = 0.15 m^2/s, $v_\perp$ = -5 m/s and $D_\perp$ = 0.3 m^2/s, $v_\perp$ = 0 m/s, respectively, while thermal diffusivities of electron and ion, $\chi_{e\perp}=\chi_{i\perp}$=1 m^2/s, are constant in the two regions. The pumping speed (S_{pump} = 50 m^3/s) is specified at an albedo with including transparency of chevron and exhaust holes in divertor cassette in front of the cryopanel.

Electron density, electron and ion temperatures at the midplan separatrix are n_e^{sep} ~ $2.9x10^{19}$ m^{-3} (n_e^{sep}/n^{GW} ~0.25), T_e^{sep} ~157 and T_i^{sep} ~309 eV, respectively, which are slightly (10-20%) smaller than those in ITER simulations [7]. At the same time, electron density at r/a ~0.95 (n_e^{edge}) of $8.3x10^{19}$ m^{-3} (n_e^{edge}/n^{GW} ~0.7) is also slightly smaller than ITER expectation [8]. Here, e-folding lengths of the SOL plasma profile are λ_{ne} =3.2 cm, λ_{Te} =0.9 cm, λ_{Ti} =1.2 cm, and that of parallel heat flux profile ($\lambda_{q//}$ = 0.4 cm) is comparable to a value from analytic model extrapolating to ITER [9].

Power loading profiles at the divertor target are evaluated, which includes heat loading due to radiation and neutral flux. Case-1 and Case-2 simulate no gas puff and medium gas puff rate of 10 Pam^3/s (Γ_{puff}= $5x10^{21}$ D/s), respectively, which are shown by broken and solid lines in Fig. 3. Here, radiation power in the main edge (9.4 -10MW) is large for the two cases due to high n_e^{edge}. When radiation power at the outer divertor is increased from 4.6 MW (Case-1) to 5.8 MW (Case-2), peak q_{div} near the outer separatrix is significantly reduced from 8.4 to 5.4 MW/m^2. This is because the plasma detachment occurs in the V-shape corner as shown in Fig. 4 (b). As a result, peak heat loads for the both cases are below handling limit for water-cooled mono-block target (15 MW/m^2) and that partially-detached divertor is achieved with medium gas puff, when radiation loss from the main plasma is relatively large (P_{rad}^{edge}/P_{out} ~32%).

Simulation results in a new geometry without private tiles at the V-shaped corner ("L-corner" case) show that peak heat load is increased to 10.8 MW/m^2 and plasma becomes attached. Thus, the V-shaped corner geometry is appropriate to reduce peak heat load near the strike-point.

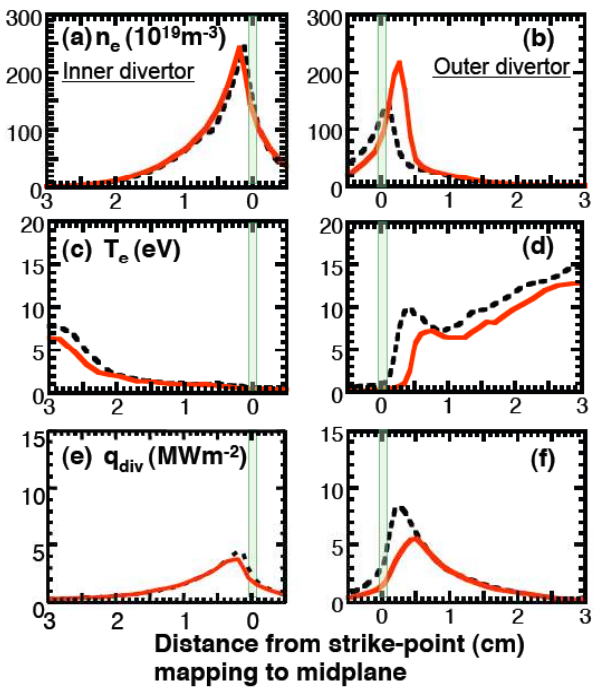

Fig.3 Electron density profiles at inner (a) and outer (b) targets, electron temperature profiles (c) and (d), target heat load (e) and (f). No gas puff (Case-1) and medium gas puff (Case-2) are shown by dotted and solid lines, respectively.

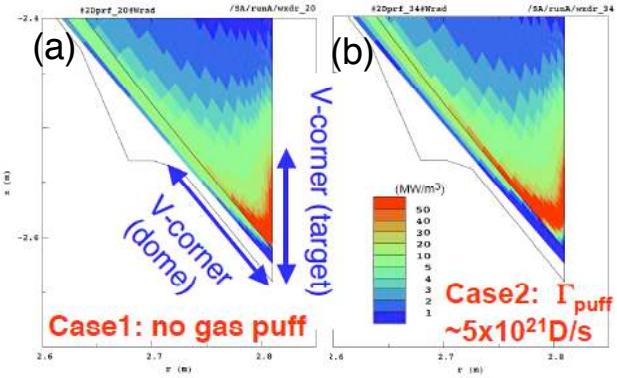

Fig.4 Radiation loss power profiles at outer divertor: (a) no gas puff (Case-1), (b) gas puff (Case-2).

Fig. 4 shows that significant radiation loss is localized (a few cm above the target), thus radiation heat load to plasma facing components in the V-shaped corner is anticipated. For the detached plasma, radiation heat load to the outer target and dome tiles is rather small (1.2 and 0.9 MW/m^2, respectively). This level is under but close to limit for CFC tiles of the private dome installed on water-cooled base. V-shaped corner design will be optimized.

4. Control of detachment and particle flow in the ITER-like divertor

Divertor plasma configuration and location of the exhaust slot are important to control the

plasma detachment. Influence of the plasma configuration on the detachment is investigated. We focus pumping fluxes in the inner and outer divertors ($\Gamma_{p,in}$ and $\Gamma_{p,out}$). Figure 5 (a) and (b) show particle (D_0 and D_2) flow, and total pumping flux (Γ_{pump} ~$1x10^{22}$ D/s) is balanced to the total flux of Γ_{out} and Γ_{puff}. Large particle flux is exhausted from the inner divertor due to short distance between the strike point and exhaust slot, while large part of the particle ($3.5x10^{22}$ D/s) are supplied to the outer divertor leg. Such "circulation" from the inner divertor to the outer divertor is seen in the ITER divertor [7], and can produce the outer divertor detachment efficiently as well as effect of the vertical target with V-shaped corner.

Particle flow pattern changes when the X-point is shifted upward by 11 cm, i.e. the outer strike point is elevated to the exhaust slot, as shown in Fig. 5(b). Pumping flux from the inner divertor and back-flow flux to the outer divertor are significantly decreased due to increase in the separation of the inner strike point. Pumping from the outer strike-point is observed. Consequently, the outer divertor plasma becomes attached while detachment of the inner divertor plasma slightly extended to the upstream. These results suggest control of the detachment at high main plasma density or under wall saturation condition: reduction in the plasma density can be established by elevation of the X-point (or change of divertor plasma configuration) as well as reducing the gas puff rate.

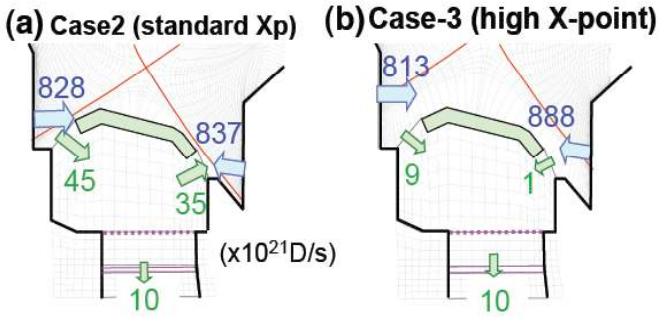

Fig. 5. Neutral flow pattern in LSN divertor calculated for (a) Case 2: standard X-point, (b) Case 3: high X-point plasmas. Unit is 10^{21} D/s. $\Gamma_{puff} = \Gamma_{out} = 5x10^{21}$ D/s for two cases.

5. Summary

JT-60SA divertor design for the ITER-like plasma configuration has been progressing. Reduction of heat load less than the handling limit can be achieved efficiently in a vertical target geometry with V-shaped corner, for relatively high n_e^{sep}~$2.9x10^{19}m^{-3}$ and main plasma radiation fraction of ~30%. Change in plasma position (elevation of outer strike-point) in the V-shaped corner affects recovery from detachment efficiently as well as reducing gas puff.

References

[1] M. Kikuchi, et al in Fusion Energy 2006 (Proc. 21st Int. Conf. Chengdu, 2006)(Vienna: IAEA) CD-ROM, FT/2-5 and http://www-naweb.iaea.org/napc/physics/FEC/FEC2006/html/index.htm.
[2] S. Sskurai, et al "Design of plasma facing component for JT-60SA", in 24th SOFT Conf. (2006), P2-F-341, submitted to Fusion Eng. Design.
[3] K. Shimizu, et al., J. Nucl. Mater. **313-316** (2003) 1277.
[4] H. Kawashima, et al., Fusion Eng. Des. **81** (2006) 1613.
[5] H. Kawashima, Plasma Fusion Res. **1** (2006) 031.
[6] D.E.Post, et al., J. Nucl. Mater. **220-222** (1995) 143.
[7] A. Kukushkin, et al. Nucl. Fusion **43** (2003) 716.
[8] A. Kallenbach, et al., J. Nucl. Mater. **337-339** (2005) 381.
[9] W. Fundamenski, et al., Nucl. Fusion **45** (2005) 950.